16th World Conference on Earthquake, 16WCEE 2017

Santiago Chile, January 9th to 13th 2017

Paper N° 2762

Registration Code: S-F1464562834

ON THE SITE EFFECT CHARACTERIZATION AT TWO URBAN STRONG-MOTION ARRAYS IN ICELAND

S. Rahpeyma(1), B. Halldorsson(2), R.A. Green(3)

(1) Ph.D. Student, Earthquake Engineering Research Centre & Faculty of Civil and Environmental Engineering, School of Engineering & Natural Sciences, University of Iceland, Selfoss, Iceland, sahar@hi.is

(2) Research Professor & Director of Research, Earthquake Engineering Research Centre. Faculty of Civil and Environmental Engineering, School of Engineering & Natural Sciences, University of Iceland, Selfoss, Iceland, skykkur@hi.is

(3) Professor, Department of Civil & Environmental Engineering, Virginia Tech Blacksburg, VA, USA, rugreen@vt.edu

Abstract

In Iceland, the most seismically active region in northern Europe, large earthquakes occur almost exclusively in two major fracture zones, the South Iceland Seismic Zone (SISZ) in the populated and cultivated farmlands of south Iceland and the mostly offshore Tjörnes Fracture Zone (TFZ) in north Iceland. Both regions are known for being densely populated and have been historically subjected to destructive near-fault earthquake strong-motions. Generally speaking, populated urban areas in Iceland consist of structures of relatively similar construction. Although site effects are generally assumed to be negligible and regionally similar, recent data collected on new strong-motion arrays, the ICEARRAY-I in Hveragerði in the SISZ and ICEARRAY-II in Húsavík in the TFZ now provide the opportunity to investigate the geological impact on site responses and study spatial distribution of ground motions. In this study, we apply the Nakamura's method using earthquake strong-motion data and microseismic measurements to assure the consistency of the results. To further investigations of geostructural influences on site responses, we present the spatial distribution maps for key parameters such as Peak Ground Acceleration (PGA) and Spectral Acceleration (SA) as a function of oscillator period as well as predominant frequency (f_0) and the relative amplification (A_0). Contrary to the fairly uniform site condition, the data exhibit variability across both arrays; however, despite the scatter of the results, we find a noticeable correlation between near surface geology and site response. Additionally, due to strong velocity reversals with depth due to repeated lava-sediment stratigraphy under most of ICEARRAY-I, we model it as a discrete dynamic structural system instead of using the body wave approximation. The results presented herein support the use of site effect investigations in combination with surface geology to improve seismic microzonation studies and also present a simple, practical and reliable strategy to model soil amplification in the presence of the velocity reversals.

Keywords: Site effect; HVSR; PGA; velocity reversal; array; Iceland.

1. Introduction

Iceland, lying astride the Mid-Atlantic Ridge where the North American and Eurasian crustal plates which are diverging at an average rate of approximately 2 cm/y, has been geologically active during the last 20-25 million years [1,2]. Running from south to north, the onshore part of the divergent plate boundary shifts eastward and is connected to the divergent segments of the Mid-Atlantic Ridge lying to the north and south by two transform fault zones: (1) the completely onshore South Icelandic Seismic Zone (SISZ) with an approximately 80 km long by 20 km wide in the south, (2) the mostly offshore Tjörnes Fracture Zone (TFZ) with around 120 km long and as much as 70 km wide in the north coast of Iceland (see Fig. 1) [3,4]. During recent decades, the seismic potential of the SISZ has been well investigated, characterized by a network of N-S right lateral strike-slip faults that produce destructive earthquakes either as strong single or sequences of events over a period lasting from weeks to years [5]. On the other hand, the TFZ in the north is known as a tectonically complex triangular area that is primarily composed of three NW-SE lineaments: Dalvík lineament, Grimsey lineament, and Húsavík Flatey Fault (HFF) [6–8]. Essentially, since the most of the TFZ is offshore, historical information and geological observations are limited so the earthquake catalogue of the TFZ is less complete and less comprehensive in comparison to the SISZ.

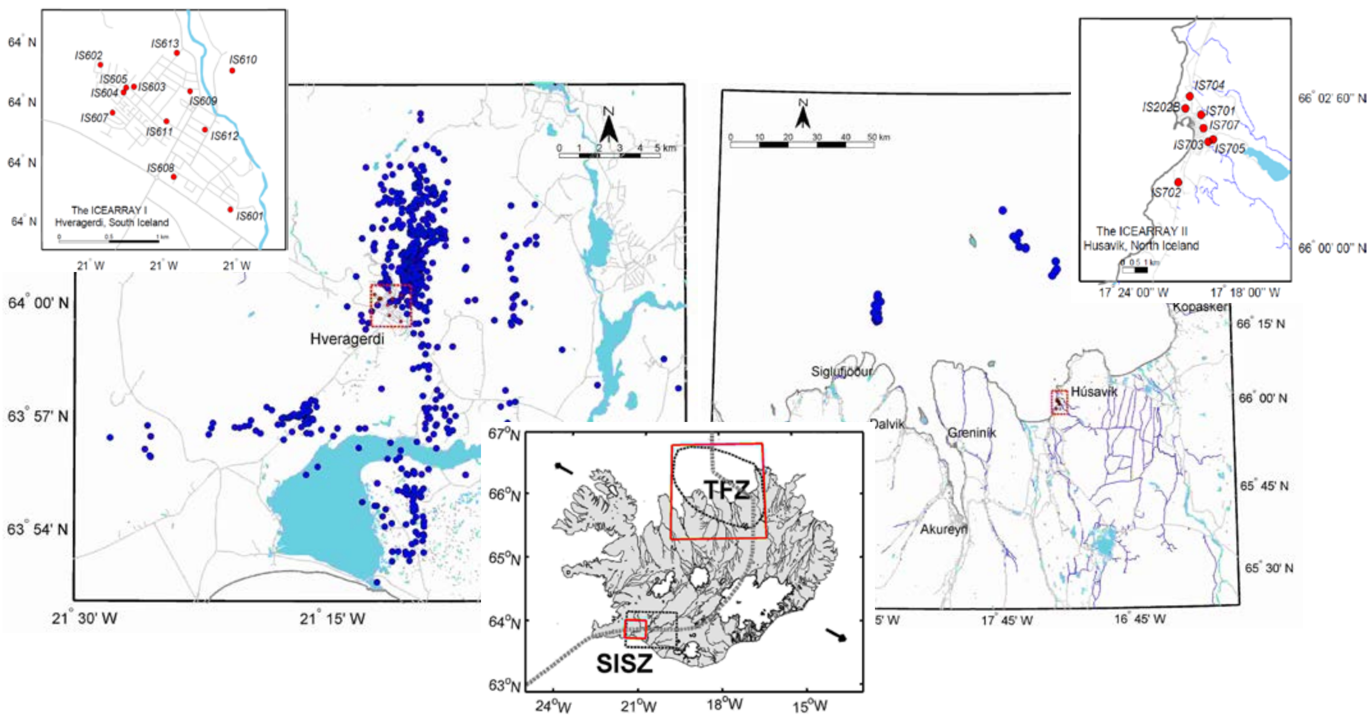

Fig. 1 The inset picture at the middle shows geodynamic map of Iceland with respect to the Mid-Atlantic Ridge (dashed gray line), the South Iceland Seismic Zone (SISZ) and the Tjörnes Fracture Zone (TFZ) outlined by the black dashed lines and pictures on the left and right are represented by red solid triangle. Picture on the left shows the aftershock distribution (blue circles) from 29 May 2008 Ölfus earthquake in southwest Iceland. The ICEARRAY-I stations (red dots) are located within the town of Hveragerði (red dashed rectangle). The inset picture at the top left shows the twelve ICEARRAY-I strong-motion stations (represented by red circle symbols, along with station ID-codes). Picture on the right shows the seismicity distribution (blue circles) for the duration of September 19, 2012 to April 4, 2013 in the TFZ, in north Iceland. The inset picture at the top right shows the seven ICEARRAY II strong motion stations (red circle symbols, along with station ID-codes) in Húsavík (represented by red dashed triangle).

Earthquake strong-motions in Iceland are monitored by the Icelandic Strong-Motion Network (ISMN) stations primarily in the SISZ and the margin of TFZ. In 2007, the first Icelandic strong-motion array (ICEARRAY-I) was deployed in the town of Hveragerði in the SISZ and consists of 12 CUSP-3Clp three-component accelerographs in an area of around 1.23 km^2 with inter-station distances ranging from 50-1900 m (Fig. 1) [9]. Subsequently, in 2012, ICEARRAY-II was set up in the town of Húsavík, the second largest urban area in the north Iceland (Fig. 1), and consists of 7 free-field stations [10]. It is noteworthy that both arrays have dramatically increased the Icelandic strong-motions dataset. During the seismic sequence starting on 29 May 2008 with the *Mw*6.3 Ölfus earthquake, ICEARRAY I recorded the strong-motions of the main-shock and more than 1700 aftershocks [11]. More recently, ICEARRAY-II recorded the strong motions from approximately 26 events during the largest earthquake sequence in the TFZ in the last 30 years.

The influence of surface topography and site conditions on the seismic waves largely accounts for the spatial variation in the amplitude and frequency content of the seismic ground-motions. In other words, localized geological settings, even over relatively small area, profoundly influence the characteristics of the seismic waves to include seismic strong-motion amplitude [12,13]. As a result, dynamic site characterization is a major aspect of geotechnical earthquake engineering due to its significant role in seismic hazard analysis. It is worth noting that the common geologic profile in Iceland consists of repeated layers of basaltic lavas with intermediate sedimentary layers [14] that leads to strong reversals in the small strain shear wave velocity with depth. It has been shown that velocity reversals significantly affect site response and therefore it should be considered in developing seismic design ground motions [15–19]. However, because of the relatively thin and easily removable topsoil in Iceland, site effects are typically (and erroneously) assumed to be negligible and spatially uniform.

Providentially, recent data collected on ICEARRAY-I and -II provide the unique opportunity to not only study the spatial distribution of ground motions, but also to estimate the localized site effects and their correlation to the complex geology in Iceland. Among several techniques to quantify the site effects, Nakamura's method, also known as Horizontal to Vertical Spectral Ratio (HVSR), is one of the most practical and well-known tools [20]. The HVSR method is based on the premise that the vertical component of the incident wave is unaffected by a geologic profile that consists of horizontally lying strata that are relatively uniform laterally.

In this study, we present the results of analyses of the recordings from ICEARRAY-I and -II. In order to estimate the localized site effects, we applied Nakamura's method using both earthquake recordings and ambient noise measurements to verify the reliability of the results. We investigated the characteristics of the geologic profiles for cases where bimodal amplification is observed in the HVSR analysis. In addition, the strong-motion amplitudes (PGA and SA) are calculated for each record and distribution patterns are quantified across both arrays. Moreover, we presented spatial distribution maps including PGA and SA (for different spectral periods), Predominant frequency, and Amplification factor. Finally, deficiency of theoretical site amplification modeling due to strong velocity reversals within depth ended up employing dynamic system modeling.

2. Data

2.1 Array strong-motion data

Following the 29 May 2008, *Mw*6.3 Ölfus earthquake in the western part of the SISZ, the ICEARRAY-I recorded over 1700 aftershocks, each on multiple stations. The main-shock was characterized by intense ground accelerations of relatively short durations (5-6 seconds) and large amplitude near-fault velocity pulses. Despite the relatively small inter-station distances across the array, noticeable variations of earthquake ground-motion amplitudes and frequency content were observed. The geometric mean of the horizontal PGA varied from about 44 to 87% g [11]. The first motions recorded during the Ölfus earthquake originated from an approximately 10 km long N-S trending fault rupture located approximately 6.5 km E-S of the town Hveragerði. However, the epicenter of the majority of the aftershocks occurred on another N-S trending fault rupture less than 2 km from the town of Hveragerði that is approximately 20 km in length (Fig. 1) [21].

After filtering the motions based on the quality of the recordings, approximately 1600 aftershocks from ICEARRAY-I were selected for analysis. The dataset is characterized by strong-motions by geometric means of the horizontal PGA in the range of 3.5~38% g from earthquakes of local magnitudes of 0.42~4.75 and epicentral distances of 1.6~15 km that occurred between May 2008 and May 2009. Furthermore, ICEARRAY-II recorded 26 earthquakes including the strongest swarm during the intense period of seismic activity in the northwestern part of the TFZ from October 2012 to April 2013. The first swarm, in October 2012, occurred on the

Eyjafjarðarâll rift and HFF, while the swarm in 2013 took place on the Grimsey Oblique Rift. The associated strong-motions are characterized by geometric means of the horizontal PGA in the range of 0.5~3.0% g from earthquakes of local magnitudes in the range 3.1~5.4 and epicentral distances around 46~74.5 km. Fig. 2 shows the ICEARRAY-I and -II database characteristics from parametric earthquake data.

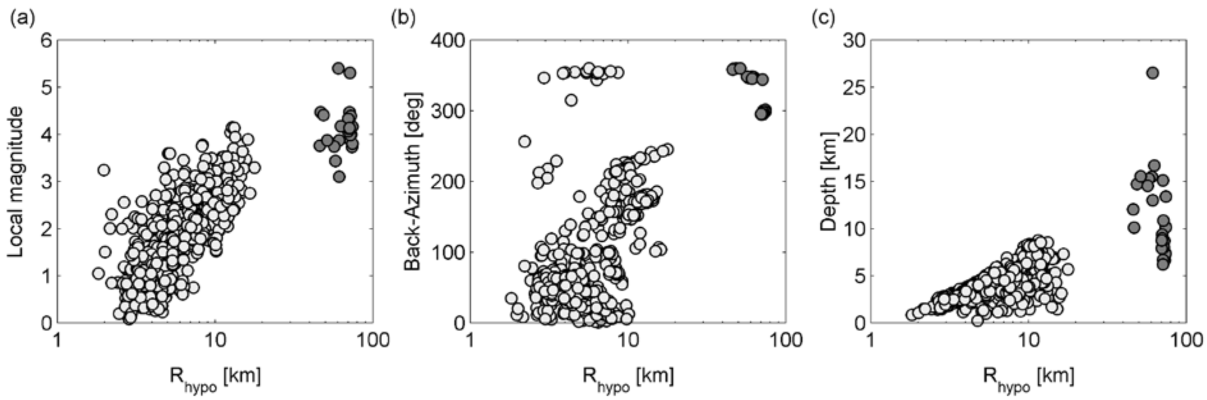

Fig. 2 Different earthquake parameters vs. hypocentral distance from strong-motion station IS605 (light gray, ICEARRAY-I) and IS705 (dark gray, ICEARRAY-II): (a) local magnitude, (b) back azimuth, and (c) depth plotted

2.2 Microseismic data

During recent decades, many researchers have examined the reliability of using ambient noise measurements, both numerically and experimentally, for quantifying of site effects [22,23]. Microseismic noise data can be easily obtained and provide practical information regarding the stratigraphy of the geological profile. Towards this end, microseismic noise at the array stations has been analyzed using HVSR method, in addition to the analysis of earthquake strong-motion recordings. Continuous ambient noise recordings of a minimum one-hour duration were performed at the ICEARRAY-I and -II sites using three-component REF TEK 130-01 Broadband Seismic Recorders and Lennartz LE-3D/5s. For sites where long recordings were available the most stable ones were split up into multiple and unique parts of 20 minutes.

3. Analysis and Results

Nakamura's method is one of the most practical approaches to investigate the amplification properties of geologic profiles. In this study, we applied the methodology recommended by Site EffectS assessment using AMbient Excitations (SESAME) research project for performing HVSR analyses [13]. In order to obtain the HV-ratio for each earthquake event, after several sensitivity analyses for selecting input parameters (e.g. smoothing coefficient, averaging method, etc.), we calculated the absolute Fourier spectrum of each of the three components over the duration of the record. The spectral amplitudes were smoothed using the Konno and Ohmachi with a smoothing coefficient of B=20 [24] for the selected bandwidth. A single smoothed spectrum representing horizontal ground motions was obtained by calculating the geometric mean of the two smoothed horizontal spectra. Dividing the spectrum for the horizontal motions by the spectrum of the vertical component produced the HVSR as a function of frequency for each event-station pair. Finally, the average HVSR and the corresponding standard deviation as a function of frequency for each station were calculated using geometric mean of HVSR from the recordings [13]. To assess the reliability and the applicability of the HVSR results from earthquake data, the same HVSR procedure was applied to the ambient noise measurements. We calculated the HVSR for each time segment and the mean HVSR and corresponding standard deviation as a function of frequency, producing the station-representative HVSR from microseismic data. Fig. 3 and Fig. 4 show the geometric mean of amplification curves and the associated $\pm 1\sigma$ for all earthquake recordings and microseismic measurements across both arrays.

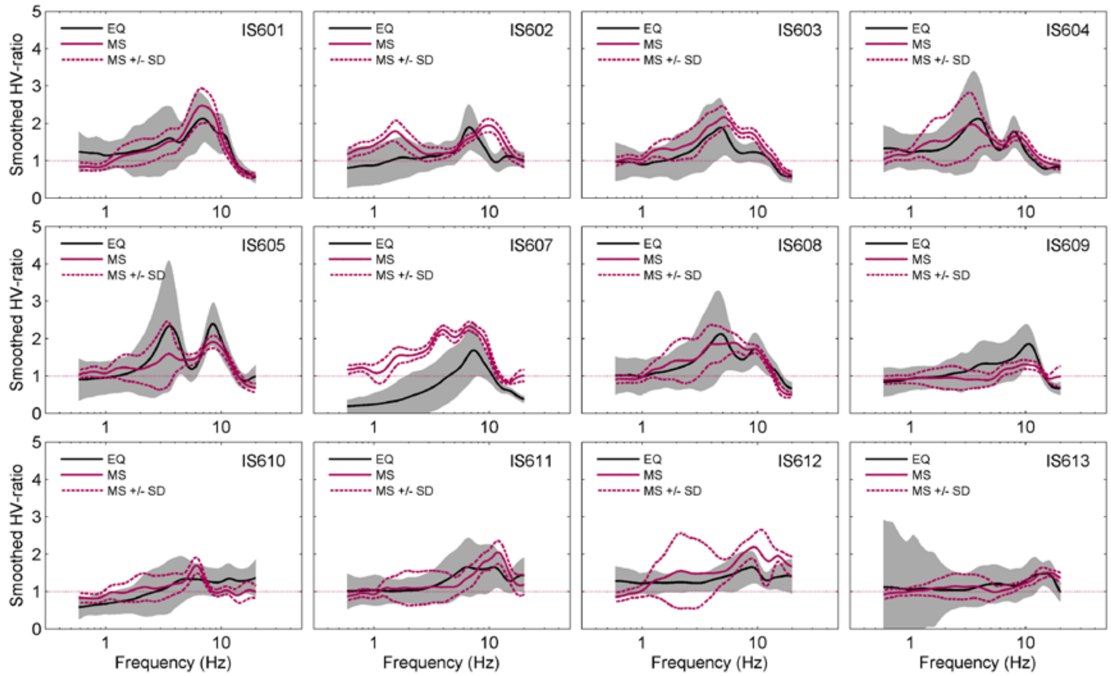

Fig. 3 Comparison of the mean HVSR estimated from earthquake and microseismic data (solid black and red lines) $\pm 1\sigma$ (gray shaded areas and red dashed line) for the twelve ICEARRAY-I stations. [17]

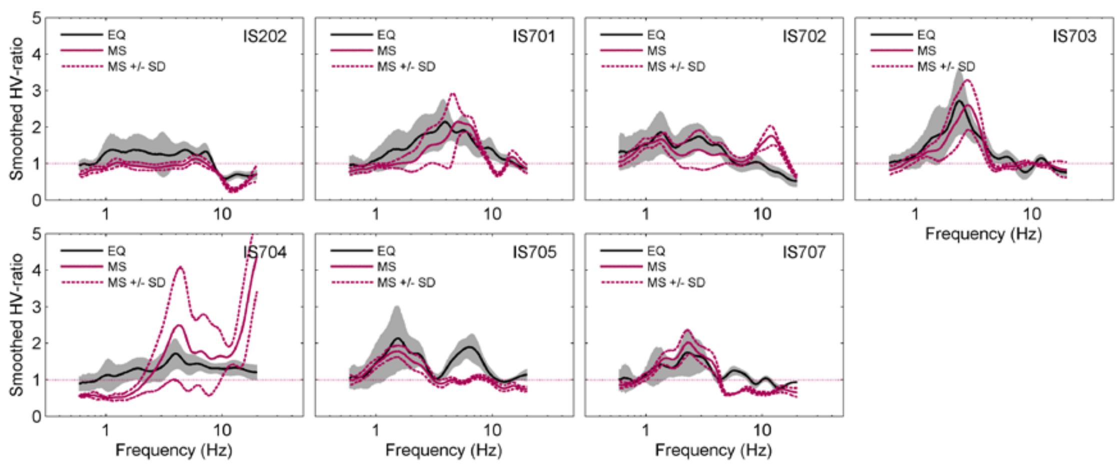

Fig. 4 Comparison of the mean HVSR estimated from earthquake and microseismic data (solid black and red lines) $\pm 1\sigma$ (gray shaded areas and red dashed line) for the seven ICEARRAY-II stations.

3.1 Topology of the HVSR results

Despite the small aperture of the Icelandic arrays, Fig. 3 and Fig. 4 show notable differences in the HVSR pattern among stations. Thus, we grouped the results into: (1) bimodal amplification curves (ICEARRAY-I: IS604, IS605, IS608; ICEARRAY-II: IS705); (2) single narrow-band peak amplification curves (ICEARRAY-I: IS602; ICEARRAY-II: IS703); (3) broad amplification curves over a wide frequency range (ICEARRAY-I: IS601, IS603, ICEARRAY-II: IS701, IS707); and finally (4) very low and uniform amplification curves across the frequency range (ICEARRAY-I: IS609-613, ICEARRAY-II: IS202, IS704). This variation in the HVSR highlights the existence of the significant site effects due to complex and varying geostructural settings within the town of Hveragerði and Húsavík.

With the exceptions of stations IS609, IS610, and IS613, which are located on a very old bedrock, the ICEARRAY-I stations are located on lava-rock layer overlying sedimentary layer. In Hveragerði, the uppermost lava layer is relatively young basaltic lava of varying thickness (10-30 meters according to boring log information). The lava layer lies on top of a sedimentary layer (of similarly varying thickness) which in turn overlies an older lava layer. No information on the thickness of the lower layer exists, but it flowed from the same volcanic fissure and based on the spatial extent of the lava it is most likely of similar thickness as the younger lava layer. From the typical layered structure of young geological formations in south Iceland, it is extremely likely that the older lava layer is underlain by another sedimentary layer. The relatively low and uniform amplification in the northeast of the ICEARRAY-I reveals that the geologic profile does not exhibit any sharp impedance contrast (e.g. IS609-613). In contrast, theoretical and numerical investigations for station IS605 in this study imply that the bimodal amplification occurs because of two large impedance contrasts, one deep and the other shallow. The same trend can be observed at IS604 which is located 54 meters southwest from IS605, indicating similar substructures. When compared with the amplification curve of station IS603, however, the difference indicates that the velocity contrast under the station is much less abrupt compared to IS603 and especially IS605. These amplification curves are in stark contrast with those at the bedrock stations, which are characterized by high frequency peaks (~10 Hz) of very low amplitudes.

In contrast to Hveragerði, the geological setting of Húsavík is generally characterized by several Pleistocene and Holocene sedimentary layers, which mainly overlie the Grjótháls lava and breccia [25,26]. More detailed investigations reveal that the subsoil structure across ICEARRAY-II can be grouped into three main regions according to the different origin and geological aspects of layers [26]. The northernmost part of the town, where stations IS202 and IS704 are located, mostly lies on Pleistocene Tillite rock. This hard layer is exposed in up to 50-meter high cliffs in Húsavíkurhöfði and most probably underlies most parts of Húsavík basin (central part of the town) [26]. The HVSR of approximately unity across the frequency range of IS704 and IS202 is representative of the hard layer underlying the sites, since compact sediments and hard rock sites generally tend to experience no significant ground amplification. The southwest of Húsavík, where station IS702 is located, is characterized as being underlain by hyaloclastites (Pleistocene Interglacial), and the stations in the central part of the town (i.e., IS701, IS703, IS705, and IS707) sit on the Lateglacial restored/horizontal sediments [26]. It should be noted that there is considerable variation in subsurface topography within the town and such geologic profiles enhance the variation in site effects and ground-motion amplitudes.

3.2 Spatial distribution of HVSR characteristics and ground-motion amplitude

In order to provide a better understanding of the localized site effects and the link with near surface geology across the arrays, the spatial distribution of fundamental frequencies, maximum amplitudes of the amplification curves, PGA, and SA for different oscillator periods using earthquake recordings are shown as surface plots in Fig. 5 and Fig. 6. Distribution of predominant frequency in ICEARRAY-I shows a clear northwest-southeast descending trend. The almost linear decreasing pattern can be explained based on geological features of the area. Stations IS609, IS613, and IS610 are located on an old bedrock while the remaining stations are located on a post-glacial lava-rock layer that overlies a sedimentary layer, according to shallow boreholes logs. Fig. 5 shows that motions from stations located on lava-rock are characterized by lower predominant frequencies and larger relative amplitudes than those on older hard bedrock. Moreover, the bimodal peaks are only observed at stations located on more complex geologic profiles (i.e., sandwiched sedimentary layers by lava-rack layers). Furthermore, the spatial distribution maps of PGA show station IS610 which is located on top of the hill has higher strong-motion amplitude in comparison to other stations. The obtained results are in good agreement with previous studies on the main-shock where stations IS607, IS602, IS602, and IS610 show larger amplitudes.

When focusing on the distribution of predominant frequency in ICEARRAY-II (Fig. 6), the results show a general north-south trend of decreasing peak predominant frequency that is in high correlation with geological settings of the area. As it is abovementioned, the northernmost part of the town lies on Pleistocene Tillite hard rock and the rest of town is mostly located on sedimentary layer. Fig. 6 shows that motions from stations located on sedimentary layer in central part of the city are characterized by lower predominant frequency with broad or multiple amplification curve and higher strong-motion amplitude (i.e. PGA and SA).

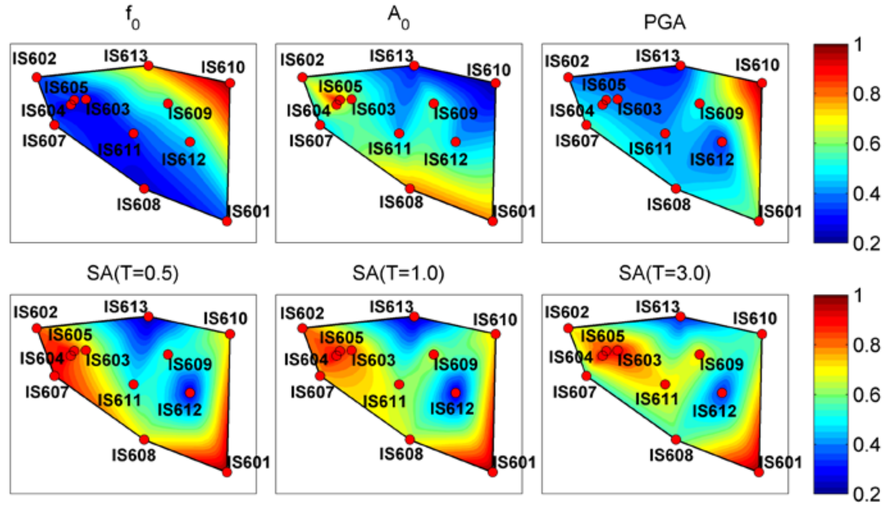

Fig. 5 Normalized spatial variability of local site effects and strong-motion amplitude in Hveragerði with the ICEARRAY I stations marked as red dots. Fundamental frequency (f_0), amplification factor (A_0), mean of PGA, SA (T=0.5, 1.0, 3.0 sec) from earthquake recordings.

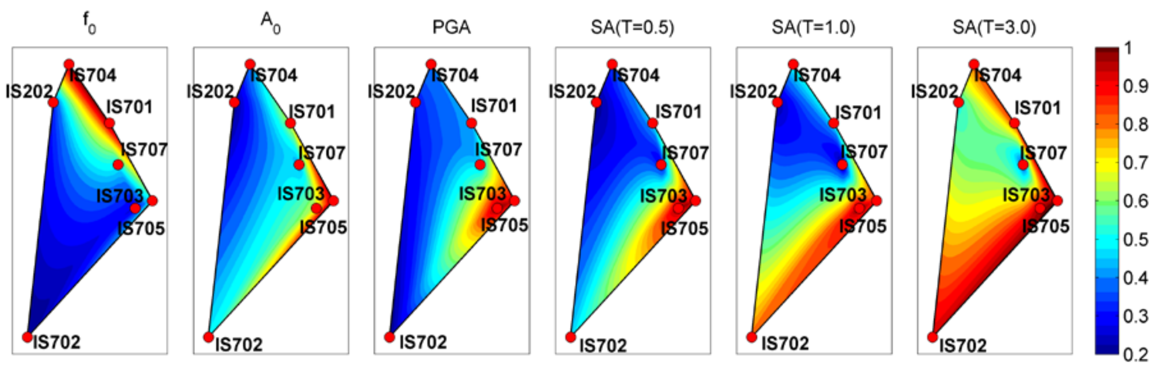

Fig. 6 Normalized spatial variability of local site effects and strong-motion amplitude in Húsavík with the ICEARRAY II stations marked as red dots. Fundamental frequency (f_0), amplification factor (A_0), PGA, SA (T=0.5, 1.0, 3.0 sec) from earthquake recordings.

3.3 Seismic parameters vs. HVSR characteristics

Theoretical and numerical investigations have shown that a sharp peak in HVSR is indicative of high impedance contrast between a softer layer overlying a stiffer layer [13,16,27]. Similarly, we interpret the bimodal amplification curve from earthquake data at station IS605 (ICEARRAY-I) and station IS705 (ICEARRAY-II) as coming from two considerable velocity contrasts at different depths, indicating a complex structure of repeated hard rock (e.g. lava, Tillite, stiff sediments)-soft sediment strata. However, the explanations for bimodal amplification curves for stations IS605 and IS705 are likely entirely different. It should be emphasized that due to small epicentral distances (less than 20 km) and high apparent velocity over the ICEARRAY-I, the waves consists exclusively of body waves with near vertical incidence angles. In contrast, the waves in ICEARRAY-II are assumed to be comprised mostly of surface waves as a result of large epicentral distance (~40-80 km) and likely lower velocity over the array.

On closer scrutiny, Fig. 3 reveals that the HVSR in station IS605 is characterized by a greater variability in the lower-frequency peak (~3-4 Hz) but less in the higher-frequency peak (~8-9 Hz) for both earthquake and microseismic data, with the level of mean amplification for both peaks being almost the same. Hence, in Fig. 7 we try to investigate the trend of the bimodal amplification curve versus different seismic parameters by clustering the aftershocks into two groups, those associated with lower (gray, Fig. 7b) and higher (cyan, Fig. 7c) predominant frequencies. Fig. 7a reveals that the two groups are comprised of aftershocks that occurred nearly equally on the two different fault structures. Furthermore, there is no azimuthal dependency of predominant frequency (Fig. 7g). Likewise, both groups of earthquakes have approximately similar coverage of hypocentral distances (Fig. 7f). Nevertheless, there is a noticeable correlation between earthquake intensity and the associated predominant frequency (Fig. 7d-e). This means that events with higher intensities generally appear to excite the lower-frequency peak. In other words, the lower predominant frequency peak is clearly observed for earthquakes of large magnitude that mainly are associated with maximum HVSR amplitude and much greater scatter in amplitude.

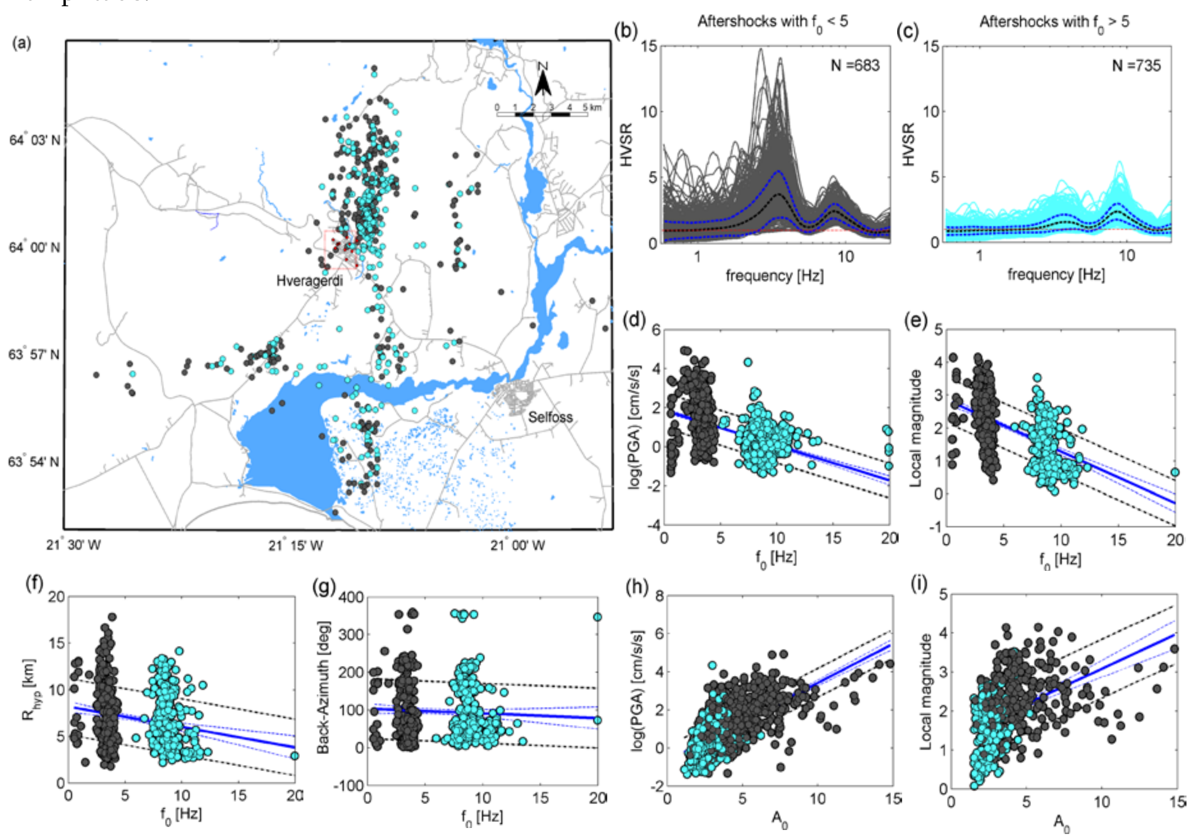

Fig. 7 (a) distribution of aftershock locations recorded by ICEARRAY-I grouped according to the predominant frequency range above (cyan) and below (gray) 5 Hz, using station IS605. The HVSR curves for two groups of aftershocks is shown in (b) and (c) as well as the mean HVSR ± 1σ, with N the number of available earthquake. Also shown the (d) PGA, (e) local magnitude, (f) hypocentral distance, and (g) back-azimuth versus the predominant frequency f_0. (h) PGA and (i) event magnitude versus Amplification factor A_0 (Gray: $f_0 \leq 5$ *Hz* and cyan: $f_0 > 5$ *Hz*). [17]

As can be seen in Fig. 4 microseismic measurements are not able to capture the shallower layer in soil structure and the soil layering filters out the high frequencies. Additionally, contrary to the ICEARRAY-I as shown in Fig. 8a, the predominant frequencies of bimodal amplification in ICEARRAY-II are highly correlated to the source of events. It is clear that low-frequency peaks are mainly associated with the 2012 swarm occurred on HFF, while the 2013 swarm that took place on the Grimsey Oblique Rift is linked to the high-frequency peaks (Fig. 8a). The significant dependency to the direction of incoming waves is clear in Fig. 8g. It is also conspicuous that events associated with lower-frequency peaks have larger hypocentral distance (Fig. 8f) and events with larger magnitude are associated with lower-frequency peaks and larger amplification.

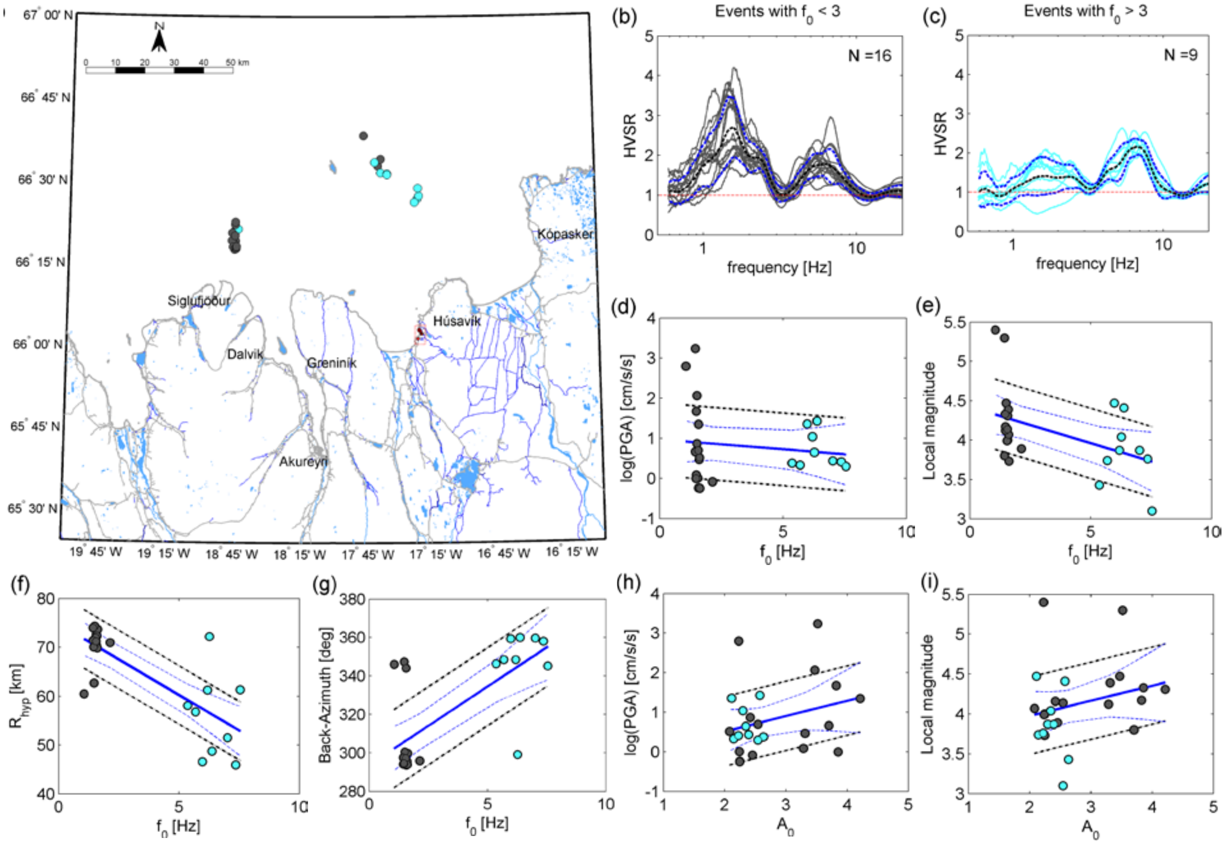

Fig. 8 (a) Map of 26 events locations recorded by ICEARRAY II grouped according to the predominant frequency range above (cyan) and below (gray) 3 Hz, using station IS705 located in the town of Húsavík (red dashed rectangle). The HVSR for the two groups of events is shown in (b) and (c) as well as the mean HVSR± 1σ, with N the number of available earthquake. Also shown the (d) PGA, (e) local magnitude, (f) hypocentral distance, (g) back-azimuth versus the predominant frequency f_0. (h) PGA, (i) event magnitude versus Amplification factor A_0 (Gray: $f_0 \leq 3$ *Hz* and cyan: $f_0 > 3$ *Hz*).

3.4 Modeling the bimodal response at stations IS605

Generally, the amplification of HVSR is interpreted by considering either surface waves or the excitation of the body wave field. It is noteworthy that the inversion of physical parameters of the subsoil structure as a function of depth on the basis of HVSR using the body wave approximation provides better results around the resonance frequency [28–30]. We however found that in general, HVSR results obtained using the body wave approximation are relatively insensitive to reverse velocity contrasts due to a hard layer overlying a softer layer. For that reason, and due to the obvious mechanical similarities to that of a dynamic structural system, we model the geologic profile as a classically damped dynamic system subjected to a base excitation [17,31,32]. Geological evidence and borehole records show the existence of two holocene lava layers under IS605 and for that reason a two-degree of freedom (2DOF) system was assumed to model the bimodal HVSR amplification curve at station IS605.

We assume the lava layers are rigid masses m_1 and m_2 (where the subscripts 1 and 2 refer to the lower and upper lava layers, respectively) and the lower and upper sedimentary layers are assumed to be massless springs having stiffnesses k_1 and k_2, respectively. Considering a unit-area vertical column of the soil profile, the mass is calculated from $m=\rho H$ (ρ: density and H: layer thickness). The shear stiffness is obtained as $k=\mu/H$ where μ is shear modulus and is calculated from $\mu=\rho\beta^2$ (β: shear wave velocity). It is noteworthy that the thickness of uppermost basaltic layer is ~10-30 m (based on borehole information) lies on top of a sedimentary layer with roughly similar thickness distribution, which in turn lies on top of an older lava layer. The boreholes are not deep enough to provide information on the lower layers. Table 1 summarizes the parameters of the final model which is schematically shown in Fig. 9(a). Solving the eigenvalue problem of the dynamic system results in fundamental frequencies of oscillation at around 3.6 Hz and 8.4 Hz, respectively, in perfect agreement with the predominant frequencies at IS605 from the HVSR analysis. For completeness, the corresponding total displacement transfer function, assuming 5% damping, is shown in Fig. 9(b).

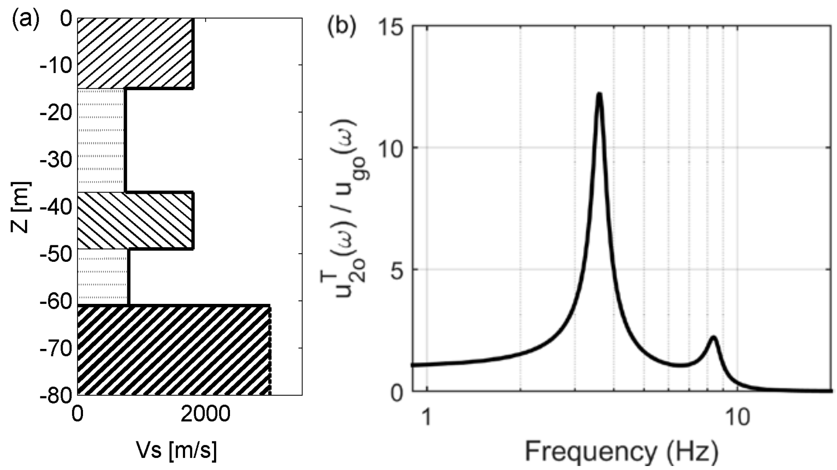

Fig. 9 (a) Shear-wave velocity profile obtained by modal analysis (hatched and dotted areas denote lava and sedimentary layers, respectively, with the bottom layer indicating bedrock). (b) The total displacement transfer function corresponding to the soil structure in (a), exhibiting two fundamental modes at the predominant frequencies.

Table 1. Soil and 2DOF model properties. [17]

Layer	Soil				2DOF system	
	$H[m]$	$\rho[g/cm^3]$	$Vs[m/s]$	$Gs[N/m^2]$	$k[N/m]$	$m\,[kg]$
Lava (L_1)	15	2.2	1800	7.13×10^9		51.7×10^3
Sediment (L_2)	22	1.7	750	0.95×10^9	43.5×10^6	
Lava (L_3)	12	2.2	1800	7.12×10^9		55.9×10^3
Sediment (L_4)	12	1.8	800	1.15×10^9	96.0×10^6	

4. Summary and Conclusion

Deployment of the ICEARRAY-I and -II, two small-aperture urban strong-motion arrays in the south and the north of the Iceland respectively, provides a unique opportunity to study many aspects of engineering seismology and especially site effects investigations. The ICEARRAY-I, consisting of 12 stations in the town of Hveragerði, recorded the earthquake strong motions and more than 1700 aftershocks associated with the 2008 Ölfus earthquake. Furthermore, ICEARRAY-II consists of 7 stations in the town of Húsavík and recorded 26 events associated with strong swarms in October 2012 and April 2013. In this study, we evaluated the geostructral impact of site responses in urban areas in Iceland using recorded data from both arrays.

We applied Nakamura's method for each strong-motion station using both earthquake data and microseismic measurements. Despite of almost uniform condition across the small area of the arrays, we observed strong variation in site responses. A comparison of the results from different datasets shows very good agreement among the mean amplification curves. This agreement indicates that in the absence of earthquake data HVSR analysis of microseismic measurements can be a practical way to map the site effects for microzonation purposes in Iceland. Moreover, mapping the spatial distribution of the predominant frequency shows that there is a strong correlation between the surface geology and the site response (i.e., f_0, A_0, PGA, and SA). In general, stations located on hard rock are characterized by low amplitude, high fundamental frequency, and low-level strong-motion amplitude, while stations located on repeated lava-sediment layers or sedimentary layers show broad or multiple peaks at relatively low frequencies.

Based on borehole information in ICEARRAY-I, the geologic profile consists of repeated lava-sediment layers, implying reversals in the small strain shear wave velocities with depth. Accordingly, we interpreted the bimodal peaks as coming from two strong velocity contrasts with depth. We showed that the mode with low-frequency peaks was mostly induced by stronger earthquakes, while the high-frequency peak was observed in both smaller and stronger earthquakes. However, the prominence of the lower frequency mode did not depend on azimuth, distance, or depth. Additionally, only the mode at higher frequencies was consistently excited by microseismic data, indicating that the microseismic noise, consisting largely of surface waves, either did not contain enough energy at the lower frequencies or did not penetrate deep enough to excite the mode at lower frequencies. In contrast, the bimodal amplification in ICEARRAY-II shows strong correlation with the source faults, direction of waves, distance, and depth. Furthermore, microseismic noise only captured the mode at lower frequencies which is highly correlated to the type of incident waves.

Due to the significant velocity reversals, modeling the bimodal amplification curves using the body-wave approximation was unsuccessful and the results did not reproduce the realistic soil properties in comparison with borehole data and other sources of information. Hence, we considered the bimodal amplification at IS605 to be the response of a soil structure consisting of two sets of lava-sedimentary layers, one on top of the other, and modeled it as a classically damped 2DOF linear oscillator. We took advantage of analytical results of the acceleration response of the top mass of a 2DOF oscillator subjected to a base (bedrock) excitation and calculated the system properties. The mass and stiffness were derived from the physical properties of the lava and sedimentary layers from typical values from literature, considering the lava layer to be a rigid mass; borehole records provided constraints on the layer thicknesses. In this way, the dynamic response of the free surface exhibited two clear fundamental modes of oscillation, one at 3-4 Hz, the other at 8-9 Hz, matching the observations. The soil structure obtained by modal analysis of two lava-soil profile is in accord with geologic mapping and borehole data.

The results of this study indicate that for lava-rock sites in Iceland characterized by considerable velocity reversals with depth, due to one or more sets of a lava-rock layer above a softer sedimentary layer, higher site amplification over a relatively narrow frequency range can be expected relative to rock sites without velocity reversals. Moreover, in such cases site characterization based on the average shear wave velocity in the uppermost 30 meters is not expected to apply. These results have important implications for earthquake resistant design considerations for structures on sites characterized by velocity reversals within depth.

5. Acknowledgements

This study was supported by the Icelandic Centre for Research (Grant of Excellence No. 141261-051), the Earthquake Engineering Research Centre (EERC) of the University of Iceland, and the Research Fund of the University of Iceland. The authors would like to acknowledge the work of Mr. Christian I. Oliveira who collected the microseismic data.

6. References

[1] Einarsson P (2008) Plate boundaries, rifts and transforms in Iceland. *Jökull* **58**, 35-58.

[2] DeMets C, Gordon RG, Angus DF, Stein S (1994) Effect of recent revisions to the geomagnetic reversal time scale on estimates of current plate motions. *Geophysical Research Letters* **21**, 2191-2194.

[3] Stefánsson R, Böðvarsson R, Slunga R, Einarsson P, Jakobsdóttir S, Bungum H, Gregersen S, Havskov J, Hjelme J, Korhonen H (1993) Earthquake prediction research in the South Iceland Seismic Zone and the SIL project. *Bulletin of the Seismological Society of America* **83**, 696-716.

[4] Guðmundsson Á, Brynjolfsson S, Jónsson MT (1993) Structural analysis of a transform fault-rift zone junction in North Iceland. *Tectonophysics* **220**, 205-221.

[5] Stefansson R, Bodvarsson R, Slunga R, Einarsson P, Jakobsdottir S, Bungum H, Gregersen S, Havskov J, Hjelme J, Korhonen H (1993) Earthquake prediction research in the South Iceland seismic zone and the SIL project. *Bulletin of the Seismological Society of America* **83**, 696-716.

[6] Saemundsson K (1974) Evolution of the axial rifting zone in northern Iceland and the Tjörnes fracture zone. *Geological Society of America Bulletin* **85**, 495-504.

[7] Einarsson P (1991) Earthquakes and present-day tectonism in Iceland. *Tectonophysics* **189**, 261-279.

[8] Stefansson R, Gudmundsson GB, Halldorsson P (2008) Tjörnes fracture zone. New and old seismic evidences for the link between the North Iceland rift zone and the Mid-Atlantic ridge. *Tectonophysics* **447**, 117-126.

[9] Halldorsson B, Sigbjörnsson R, Schweitzer J (2009) ICEARRAY: the first small-aperture, strong-motion array in Iceland. *J Seismol* **13**, 173-178.

[10] Halldorsson B, Jónsson S, Papageorgiou AS, Green RA, Kalogeras I, Avery H, Ólafsson S, Remseth S, Oliveira CI, Polat O, Sigbjörnsson R (2012) ICEARRAY II: A new multidisciplinary strong-motion array in North Iceland. In *15th World Conference on Earthquake Engineering (15WCEE)*, Lisbon, Portugal, Paper no. 2567.

[11] Halldorsson B, Sigbjörnsson R (2009) The M_w6.3 Ölfus earthquake at 15:45 UTC on 29 May 2008 in South Iceland: ICEARRAY strong-motion recordings. *Soil Dynamics and Earthquake Engineering* **29**, 1073-1083.

[12] Aki K (1993) Local site effects on weak and strong ground motion. *Tectonophysics* **218**, 93-111.

[13] Bard PY, SESAME-Team (2005) Guidelines for the implementation of the H/V spectral ratio technique on ambient vibrations: measurements, processing, and interpretations. SESAME European research project. *SESAME European research project*.

[14] Einarsson Þ, Douglas G (1994) *Geology of Iceland: rocks and landscape*, Mál og menning, Reykjavík, Iceland.

[15] Bessason B, Kaynia AM (2002) Site amplification in lava rock on soft sediments. *Soil Dynamics and Earthquake Engineering* **22**, 525-540.

[16] Giacomo DD, Gallipoli MR, Mucciarelli M, Parolai S, Richwalski SM (2005) Analysis and Modeling of HVSR in the Presence of a Velocity Inversion: The Case of Venosa, Italy. *Bulletin of the Seismological Society of America* **95**, 2364-2372.

[17] Rahpeyma S, Halldorsson B, Oliveira CI, Green RA, Jónsson S (2016) Detailed site effect estimation in the presence of strong velocity reversals within a small-aperture strong-motion array in Iceland. *Soil Dynamics and Earthquake Engineering* **89**, 136-151.

[18] Halldorsson B, Olivera CI, Rahpeyma S, Ólafsson S, Green RA, Snæbjörnsson JT (2016) On the HVSR estimation at Icelandic strong-motion stations. In *Proceedings of the Nordic Geotechnical Meeting* Icelandic Geotechnical Society, Reykjavík, Iceland, pp. 1243-1252.

[19] Snæbjörnsson JT, Rahpeyma S, Halldorsson B, Sigtryggsdóttir FG (2016) Effects of soil-structure interaction on the excitation and response of RC buildings subjected to strong-motion. In *Proceedings of the Nordic Geotechnical Meeting* Icelandic Geotechnical Society, Reykjavík, Iceland, pp. 1232-1242.

[20] Nakamura Y (1989) A method for dynamic characteristics estimation of subsurface using microtremor on the ground surface. *Quarterly Report of Railway Technical Research Institute* **30**, 25-33.

[21] Sigbjörnsson R, Snæbjörnsson JT, Higgins SM, Halldorsson B, Ólafsson S (2009) A note on the Mw 6.3 earthquake in Iceland on 29 May 2008 at 15:45 UTC. *Bull Earthquake Eng* **7**, 113-126.

[22] Bard PY (1998) Microtremor measurements: A tool for site effect estimation? In *Proceeding of the Second International Symposium on the Effects of Surface Geology on Seismic Motion. Yokohama, Japan*, pp. 1251-1279.

[23] Pilz M, Parolai S, Leyton F, Campos J, Zschau J (2009) A comparison of site response techniques using earthquake data and ambient seismic noise analysis in the large urban areas of Santiago de Chile. *Geophysical Research Letters* **178**, 713-728.

[24] Konno K, Ohmachi T (1998) Ground-motion characteristics estimated from spectral ratio between horizontal and vertical components of microtremor. *Bulletin of the Seismological Society of America* **88**, 228-241.

[25] Sæmundsson K, Karson JA (2006) *Stratigraphy and tectonics of the Húsavík-Western Tjörnes Area*, Iceland Geosurvey.

[26] Waltl P, Halldorsson B, Pétursson HG, Fiebig M, Sigbjörnsson R (2014) The geological and urban setting of Húsavík, North Iceland, in the context of Earthquake Hazard and Risk Analysis. In *Proceedings of the 2nd European Conference on Earthquake and Engineering Seismology (2ECEES)*, Istanbul, Turkey.

[27] Nakamura Y (2008) On the H/V spectrum. In *Proceedings of the 14th World Conference on Earthquake Engineering*, Beijing, China.

[28] Tsai NC (1970) A Note on the Steady-State response of an Elastic Half-Space. *Bulletin of the Seismological Society of America* **60**, 795-808.

[29] Herak M (2008) ModelHVSR—A Matlab® tool to model horizontal-to-vertical spectral ratio of ambient noise. *Computers & Geosciences* **34**, 1514-1526.

[30] Albarello D, Lunedei E (2010) Alternative interpretations of horizontal to vertical spectral ratios of ambient vibrations: new insights from theoretical modeling. *Bulletin of Earthquake Engineering* **8**, 519-534.

[31] Chopra AK (1981) *Dynamics of structures, a primer*, Earthquake Engineering Research Institute, Berkeley, California.

[32] Yoshida N (2015) *Seismic Ground Response Analysis*, Springer Netherlands, Dordrecht.